Cell Reports, Volume *26*

Supplemental Information

Proximodistal Organization of the CA2 Hippocampal Area

Ivan Fernandez-Lamo, Daniel Gomez-Dominguez, Alberto Sanchez-Aguilera, Azahara Oliva, Aixa Victoria Morales, Manuel Valero, Elena Cid, Antal Berenyi, and Liset Menendez de la Prida

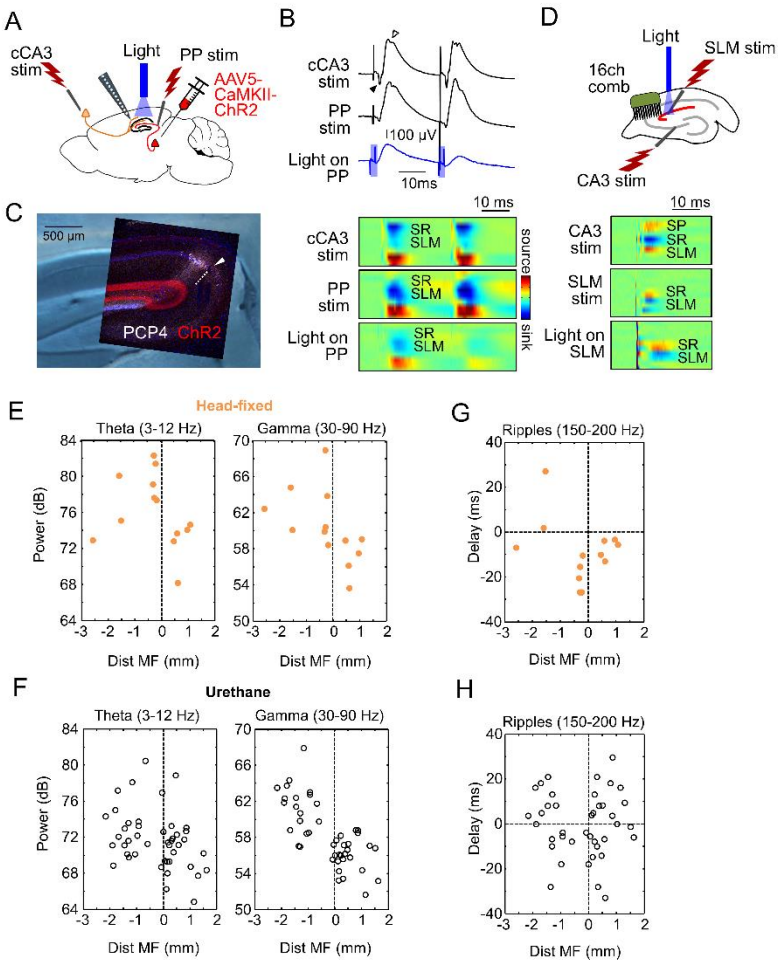

Figure S1. Electrophysiological features around CA2. Related to Figure 1.

(A) The CA2 region was targeted in vivo guided by spontaneous LFP signals and characteristic responses to stimulation of both the contralateral CA3 (cCA3) and perforant pathway (PP). The probe position was histologically validated after experiments. In a subset of animals, we used optogenetics to validate CA2 responses to PP stimulation. To this purpose, rats were injected with AAV5-CaMKII-ChR2 in the medial entorhinal cortex 3 weeks before experiments.
(B) In the SP of CA2, cCA3 stimulation elicited an antidromic spike (black arrowhead) followed by an orthodromic spike of variable amplitude (open arrowhead). PP electrical stimulation evoked a clear synaptic event typically associated to a small orthodromic response. These two characteristics aided us in targeting CA2 precisely. Optogenetic stimulation of entorhinal inputs elicited similar synaptic responses in CA2 than PP electrical stimulation, but the orthodromic spike was less reliably elicited. Current source density (CSD) signals are shown below traces. Note similar CSD sinks at SLM after electrical and optical stimulation of entorhinal terminals. All data from the same rat.
(C) Histological validation of the experiment shown in B. The CA2 region was identified with immunostaining for PCP4. Note the probe track indicated (discontinuous line and arrowhead). ChR2 was expressed both in layers II and III of the entorhinal cortex, but only ECII stellate cell terminals project to CA2.
(D) In vitro recordings to validate CA2 responses to SLM stimulation in one rat injected with AAV5-CaMKII-ChR2 in the medial entorhinal cortex. A 16-channel silicon comb was used to record laminar signals. The CSD profile is shown at bottom. Note similar CSD responses to electrical and optical stimulation of the entorhinal terminals at SLM.
(E) Individual spectral area of the theta (3-12 Hz) and gamma bands (30-90 Hz) plotted as a function of electrode distance to MF as measured in head-fixed conditions. Data from n=12 recordings from n=5 drug-free rats.
(F) Same for data obtained under urethane (52 recording locations from n=30 urethane anesthetized rats).
(G) Delay between the ripple and SPW peaks as a function of recording location. Data from n=13 recordings from n=5 drug-free rats.
(H) Same for data obtained under urethane (52 recording locations from n=30 urethane anesthetized rats)

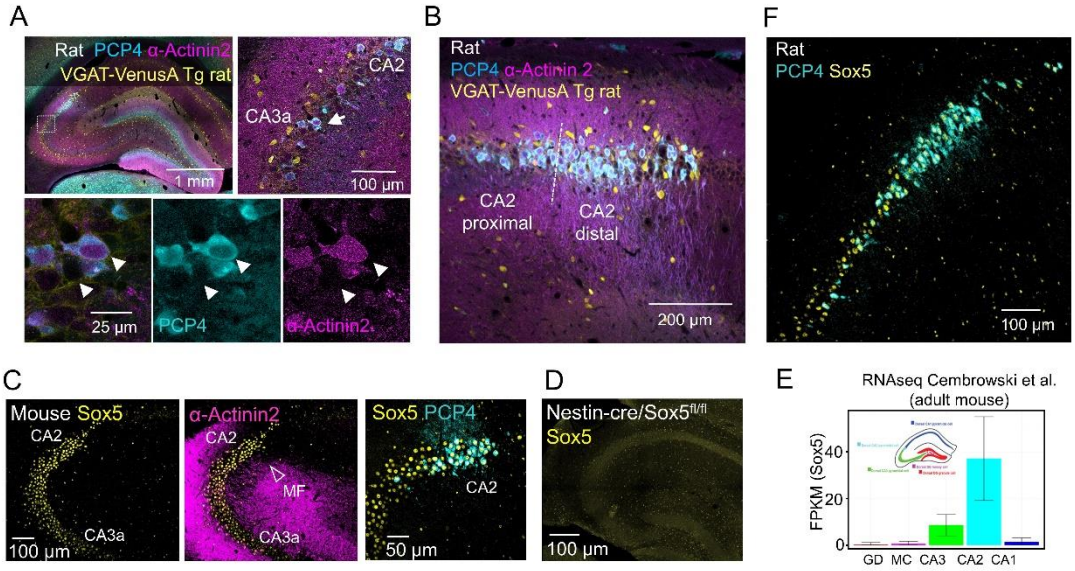

Figure S2. Proximodistal heterogeneity around CA2. Related to Figure 2.

(A) Double immunostaining against α-Actinin2 and PCP4 as evaluated in coronal sections from VGAT-VenusA transgenic rats. α-Actinin2 and PCP4 co-localized in CA2 pyramidal cells. Note some PCP4+ cells dispersed in CA3a (enlarged box shown at right). Bottom images show details of a PCP4+ and a PCP4- cell from CA3a that differ in their intensity of α-Actinin2 signal.
(B) Co-localization between α-Actinin2 and PCP4 in the CA2 region (one confocal optical section from a VGAT-VenusA rat).
(C) Immunohistochemical expression of Sox5 in a representative section from an adult mouse (one confocal section) co-localized with α-Actinin2 and PCP4. In mouse α-Actinin2 is mildly expressed at the somata.
(D) Validation of the rabbit Sox5 polyclonal antibody tested in a brain coronal section from a Nestin-cre/Sox5$^{fl/fl}$ mutant mouse.
(E) Quantitative regional RNAseq data from Hipposeq (Cembrowski et al., 2016).
(F) Co-localization between PCP4 and Sox5 in rat.

Table S1. Intrinsic properties of single cells recorded in vivo. Related to Figure 2.

	PCP4-/Thorn n=5	PCP4+ n=10	Wfs1+ n=9	GLM (P-value)			
				Cell-type	Distance to MF	Distance to SR	All factors
Resting potential (mV)	-59.7 ± 3.4	-58.7 ± 4.2	-60.5 ± 5.9	0.7124	0.2373	0.9689	0.4855
Input resistance (MΩ)	20.1 ± 11.1	20.4 ± 9.5	36.3 ± 16.2	**0.0249**	**0.0185**	0.2510	**0.0246**
Membrane time constant (ms)	8.9 ± 4.2	6.6 ± 5.5	10.9 ± 3.8	0.1782	0.2214	0.4262	0.2859
Sag amplitude @-0.3nA (mV)	0.59 ± 0.27	1.08 ± 0.51	1.08 ± 0.47	0.1327	**0.0421**	0.2430	**0.0494**
Max firing rate @0.3nA (Hz)	5.7 ± 2.4	7.8 ± 4.1	20.4 ± 10.1	**0.0006**	**0.0006**	0.8055	**0.0021**
Firing rate adapt @0.3nA	0.52 ± 0.08	0.63 ± 0.02	0.65 ± 0.04	**0.0018**	**0.0205**	0.5592	0.0514
Bursting Index	0.10 ± 0.20	0.08 ± 0.18	0.046 ± 0.09	0.7902	0.4792	0.6983	0.6870
AP threshold (mV)	-53.5 ± 4.2	-49.5 ± 3.2	-48.1 ± 4.4	0.0632	0.0520	0.5128	0.1360
AP half-width (ms)	0.94 ± 0.13	0.93 ± 0.14	0.95 ± 0.16	0.9310	0.9362	0.8130	0.9706
AHP amp (mV)	2.9 ± 1.5	3.4 ± 1.6	5.4 ± 1.8	**0.0182**	**0.0106**	0.1959	**0.0254**

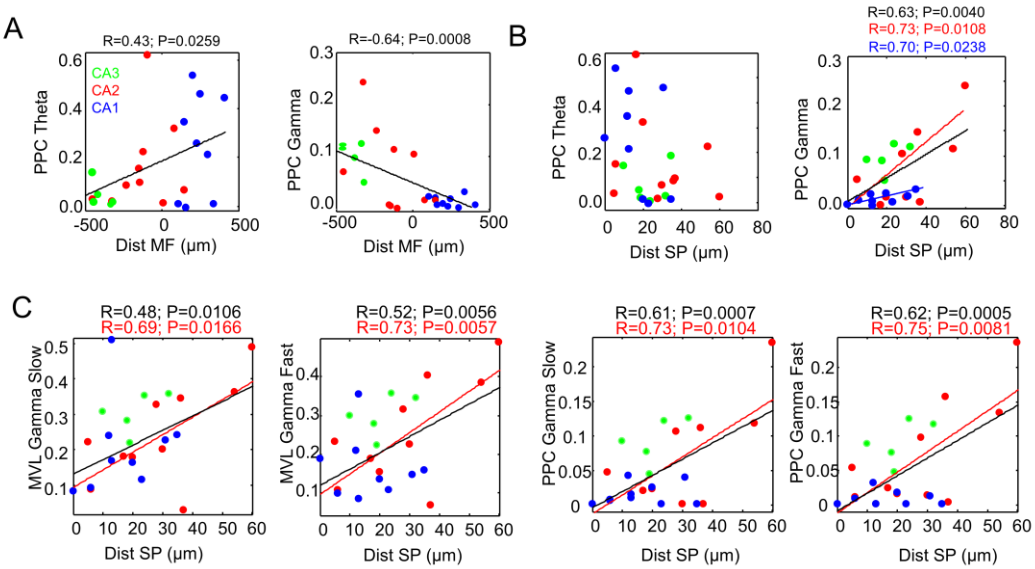

Figure S3. Phase locked firing of morphologically identified single cells. Related to Figure 3.

(A) Modulation strength calculated from the PPC index.
(B) Distribution of the PPC modulation strength as a function of the cell distance within SP. Note strong deep-superficial trends for gamma activity within the CA2 and CA1 subgroups, and for all grups together. The SP border with SP is at 0 (superficial).
(C) Modulation strength during slow and fast gamma activities as a function of the deep-superficial location of recorded cells.

Table S2. Theta and gamma modulation of single cells recorded in vivo. Related to Figure 3

All cells in the database							
	PCP4-/Thorny n=5	PCP4+ n=10	Wfs1+ n=9	GLM (P-value)			
				Cell-type	Dist to MF	Dist to SR	All factors
Theta autocorrelation index	0.38 ± 0.03	0.38 ± 0.07	0.36 ± 0.05	0.4785	0.11611	**0.00328**	**0.00756**
Theta index (MVL)	0.17 ± 0.13	0.29 ± 0.16	0.45 ± 0.27	**0.0201**	**0.01528**	0.27042	**0.02176**
Gamma index (MVL)	0.30 ± 0.09	0.24 ± 0.13	0.18 ± 0.09	0.2708	**0.04298**	**0.00761**	**0.00313**
Theta phase (rad)	1.80 ± 0.91	0.45 ± 1.07	-2.56 ± 0.72	**<0.0001**	**<0.0001**	**0.0389**	**<0.0001**
Gamma phase (rad)	3.09 ± 0.53	2.76 ± 1.03	2.74 ± 1.01	0.8737	0.6495	0.1145	0.2266
Theta phase (deg)	103.3 ± 52.2	140.2 ± 61.2	-126.9 ± 1.03	**<0.0001**	**<0.0001**	**0.0389**	**<0.0001**
Gamma phase (deg)	177.4 ± 30.5	158.4 ± 58.6	157.1 ± 57.9	0.8737	0.6495	0.1145	0.2266
Theta index (PPC)	0.04 ± 0.06	0.16 ± 0.18	0.25 ± 0.21	0.1477	**0.04250**	0.18519	**0.04060**
Gamma index (PPC)	0.091 ± 0.026	0.067 ± 0.075	0.0108 ± 0.009	**0.0265**	**<0.0001**	**<0.0001**	**<0.0001**
Only cells recorded against CA1 LFP							
	PCP4-/Thorny n=4	PCP4+ n=5	Wfs1+ n=8	Cell-type	Dist to MF	Dist to SR	All factors
Theta autocorrelation index	0.38 ± 0.03	0.41 ± 0.08	0.35 ± 0.05	0.3223	0.1767	**0.0413**	0.0681
Theta index (MVL)	0.16 ± 0.15	0.28 ± 0.19	0.41 ± 0.26	0.2109	**0.0383**	0.1391	**0.0373**
Gamma index (MVL)	0.30 ± 0.06	0.25 ± 0.16	0.19 ± 0.09	0.2516	0.0506	**0.0017**	**0.0016**
Theta phase (rad)	2.07 ± 0.95	1.89 ± 1.06	-2.76 ± 0.75	**<0.0001**	**<0.0001**	0.0664	**<0.0001**
Gamma phase (rad)	-3.08 ± 0.56	2.76 ± 0.74	2.56 ± 1.04	0.4633	0.4222	0.0669	0.1196
Theta phase (deg)	118.6 ± 54.6	108.6 ± 60.9	-150.3 ± 42.8	**<0.0001**	**<0.0001**	0.0664	**<0.0001**
Gamma phase (deg)	-176.9 ± 32.3	158.2 ± 42.3	147.1 ± 59.5	0.4633	0.4222	0.0669	0.1196
Theta index (PPC)	0.04 ± 0.06	0.11 ± 0.13	0.21 ± 0.19	0.2108	**0.0345**	0.2350	**0.0480**
Gamma index (PPC)	0.093 ± 0.034	0.081 ± 0.096	-0.005 ± 0.038	**0.0237**	**<0.0001**	**<0.0001**	**<0.0001**

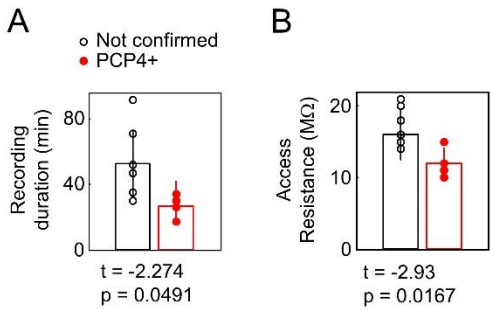

Figure S4. Effect of cell dialysis on immunoreactivity to PCP4. Related to Figure 5.

(A) Significant difference of recording duration of PCP4+ cells versus cells with non-confirmed immunoreactivity suggest dialyzing of cytoplasmic content is a major factor against neurochemical confirmation of CA2 cells with whole-cell patch recordings in vitro. Data from n=7 not confirmed cells, n=4 PCP4+ CA2 pyramidal cells. Results from a Student t-test are shown at bottom.
(B) Significant difference of access resistance through the patch pipette in PCP4+ cells versus cells with non-confirmed immunoreactivity.

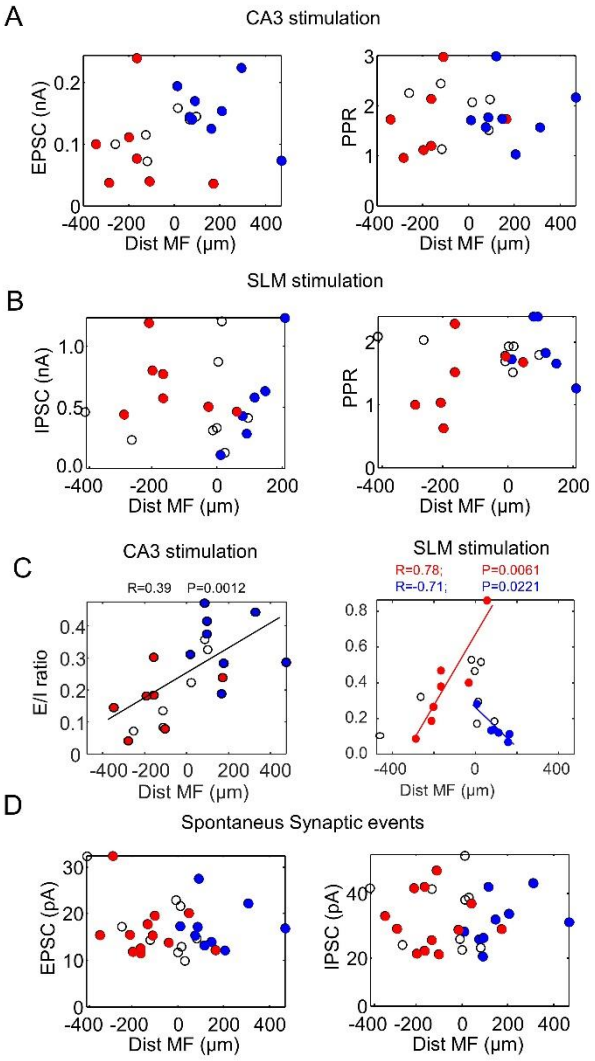

Figure S5. Synaptic activity of CA2 pyramidal cells recorded in vitro. Related to Figure 5.

(A) Relationship between the amplitude of the CA3-evoked EPSCs and paired-pulse ration (PPR) with the distance to MF. Cells without thorny excrescences and not confirmed with PCP4 (red) or Wfs1 (blue) immunostaining are shown in black. Data from n=6 not-confirmed cells, n=7 PCP4+ CA2 pyramidal cells and n=8 Wfs1+ CA1 pyramidal cells.
(B) Proximodistal distribution of the amplitude of SLM-evoked IPSCs and PPR. Data from n=6 not-confirmed cells, n=7 PCP4+ CA2 pyramidal cells and n=6 Wfs1+ CA1 pyramidal cells.
(C) E/I and I/E ratio for CA3 and SLM stimulation.
(D) Distribution of the amplitude of spontaneous EPSCs and IPSCs with the cell proximo-distal position. Data from n=9 not-confirmed cells, n=12 PCP4+ CA2 pyramidal cells and n=9 Wfs1+ CA1 pyramidal cells.

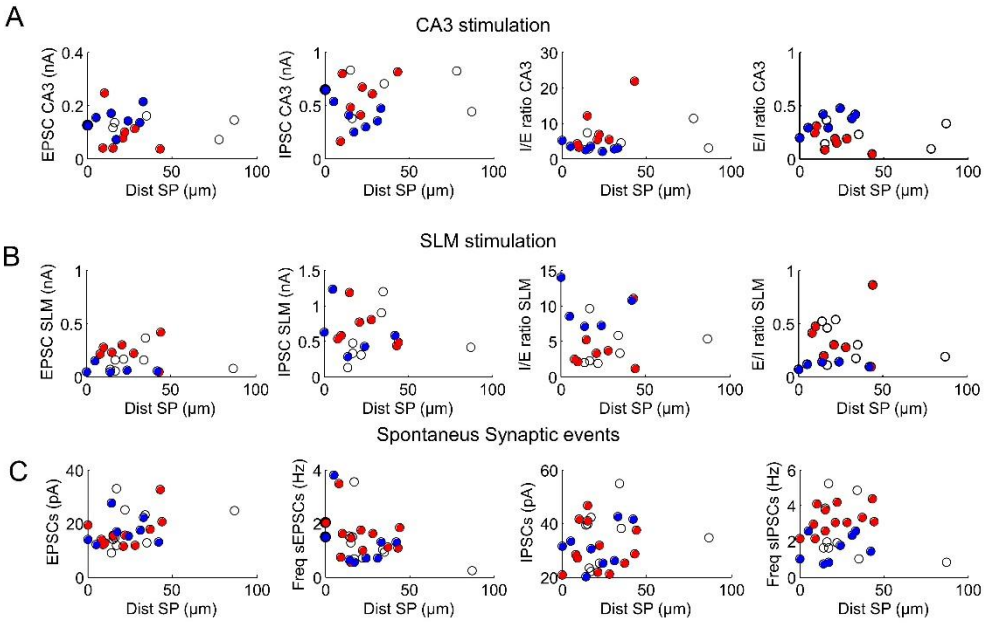

Figure S6. Relationship between synaptic currents and the cell location within SP (deep-superficial axis). Related to Figure 5.

(A) Individual data for synaptic currents evoked by CA3 stimulation plotted as a function of cell location within the SP layer. Same data as before.
(B) Same for synaptic currents evoked by stimulation at the SLM layer.
(C) Same for the amplitude and frequency of spontaneous events.

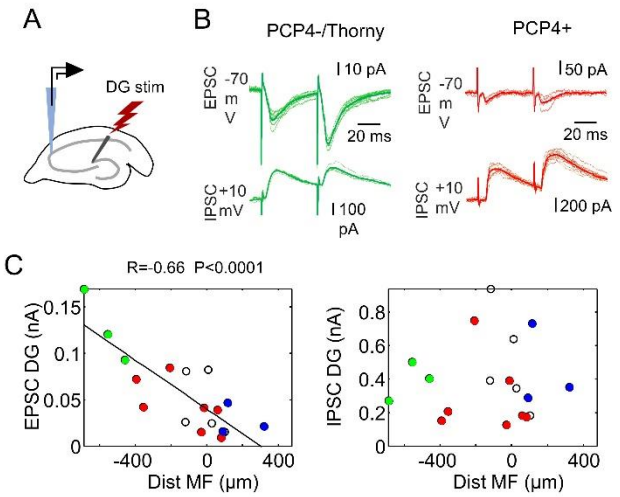

Figure S7. Responses to MF stimulation. Related to Figure 5.

(A) MF were stimulated at the upper blade tip of the DG.
(B) Examples of a CA3 and CA2 pyramidal cell repsonses to MF stimulation.
(C) Individual data for synaptic currents evoked by MF stimulation plotted as a function of the proximodistal cell location. Data from n=3 CA3a pyramidal cells, n=7 PCP4+ CA2 cells and n=3 Wfs1+ CA1 cell. In n=4 cells immunoreactivity to Wfs1 and PCP4+ was not confirmed (no thorny excrescences).